Variability in HIV-1 Transmitted/Founder Virus Susceptibility to Combined APOBEC3F and APOBEC3G Host Restriction

HIV-1 Transmitted/Founder Susceptibility to APOBEC3 Host Restriction

Amit Gaba[1*], Maria Yousefi[1 ¶], Shreoshri Bhattacharjee[1 ¶], Linda Chelico[1, *]

[1] Department of Biochemistry, Microbiology, and Immunology, College of Medicine, University of Saskatchewan, Saskatoon, Saskatchewan, Canada.

¶These authors contributed equally to this work.

*Corresponding authors

Email: linda.chelico@usask.ca (LC), amit.gaba@usask.ca (AG)

Abstract

Several APOBEC3 enzymes restrict HIV-1 replication by deaminating cytosine to form uracil in single-stranded proviral (-)DNA. However, HIV-1 Vif binds to APOBEC3 enzymes and counteracts their activity by inducing their proteosomal degradation. This counteraction by Vif is not complete as evidenced by footprints of APOBEC3-mediated mutations within integrated proviral genomes of people living with HIV-1. The APOBEC3 enzymes are co-ordinately expressed in $CD4^{+}$T cells and relative contributions of APOBEC3s in HIV-1 restriction is not fully understood. In this study, we investigated the activity of co-expressed APOBEC3F and APOBEC3G against HIV-1 Subtype B and Subtype C Transmitted/Founder viruses. APOBEC3F and APOBEC3G when co-expressed were previously determined to form a hetero-oligomer that enables partial resistance of APOBEC3F to Vif-mediated degradation. Here, we determined that that APOBEC3F interacts with APOBEC3G through its N-terminal domain. We provide evidence that this results in protection from Vif-mediated degradation because the APOBEC3F N-terminal domain contains residues required for recognition by Vif. We also found subtype specific differences in activity of Transmitted/Founder Vifs against APOBEC3G and the APOBEC3F/APOBEC3G hetero-oligomer. HIV-1 Subtype C Vifs were more active in counteracting APOBEC3G compared to HIV-1 Subtype B Vifs when APOBEC3G was expressed alone. However, HIV-1 Subtype C Vifs were less active against APOBEC3G when APOBEC3F and APOBEC3G were co-expressed. Consequently, when APOBEC3F and APOBEC3G were expressed together HIV-1 Subtype C viruses showed a decrease in relative infectivity compared to that when APOBEC3G was expressed alone. Inspection of Vif amino acid sequences revealed that that differences in amino acids adjacent to conserved sequences influenced the Vif-mediated APOBEC3 degradation ability. Altogether, the data provide a

possible mechanism for how combined expression of APOBEC3F and APOBEC3G could contribute to mutagenesis of HIV-1 proviral genomes in the presence of Vif and provide evidence for variability in the Vif-mediated degradation ability of Transmitted/Founder viruses.

Author Summary

APOBEC3 enzymes act as barriers to HIV infection by inducing cytosine deamination in proviral DNA, but their effectiveness is hindered by their counteraction by HIV Vif, which leads to APOBEC3 proteasomal degradation. The APOBEC3-Vif interaction has largely been determined using lab adapted HIV-1 Subtype B viruses and with singular APOBEC3 enzymes. Here we examined how primary isolates of HIV-1 replicated in the presence of APOBEC3F and APOBEC3G. APOBEC3F and APOBEC3G interact and this imparts partial resistance to Vif-mediated degradation. We determined that APOBEC3F interacts with APOBEC3G through its N terminal domain, and that APOBEC3F, like APOBEC3G has Vif-mediated degradation determinants in the N-terminal domain, providing a rational for protection from Vif-mediated degradation. We also demonstrate subtype-specific differences in the activity of Transmitted/Founder Vifs against APOBEC3G and the APOBEC3F/APOBEC3G hetero-oligomer. Through an analysis of Vif amino acid sequences, we identified variations influencing the Vif-mediated APOBEC3 degradation ability. This research uncovers previously unidentified mechanisms by which combined expression of APOBEC3F and APOBEC3G may contribute to HIV-1 proviral genome mutagenesis in the presence of Vif and emphasizes the contribution of amino acid variation outside of previously identified conserved regions in Vif-mediating APOBEC3 degradation.

Introduction

The APOBEC3 (A3) enzymes belong to a family of cytosine deaminases that in primates and humans has at least seven members (A3A-A3H, excluding E) (1). These enzymes act as host restriction factors against retroelements, retroviruses, and DNA viruses (2-4). APOBEC3 enzymes deaminate cytosine to uracil in single-stranded (ss) DNA replication intermediates, which induces mutations in or degradation of DNA, as well as inhibiting retroelement and retroviral reverse transcriptase through a deamination-independent mechanism (2-6).

Out of the seven human A3 family members, five (A3C S188I, A3D, A3F, A3G and A3H (Haplotypes II, V, and VII)) have been reported to inhibit HIV-1 in absence of its Vif protein (7-12). Vif induces degradation of A3 enzymes through the proteasome (13). In the absence of HIV Vif, APOBEC3 enzymes can become encapsidated into budding virions by binding RNAs that are also bound by HIV Gag, such as HIV genomic RNA (14, 15). When these virions infect new cells, A3 enzymes will deaminate cytosines to uracils on HIV single-stranded (-)DNA, resulting in G-to-A mutations in the (+) DNA and the creation of a non-functional provirus (4). Vif acts to prevent this restriction activity by acting as the substrate adaptor in a Cullin RING ligase-5 (CRL5) E3 ligase complex, which binds A3 enzymes through Vif and results in their polyubiquitination and degradation through the 26S proteasome (13). Specifically, HIV-1 Vif becomes complexed with the scaffold protein Cullin 5, Elongin C, and the co-transcription factor CBF-β (13). The Cullin 5 binds Ring finger protein Rbx2 and Elongin C is an obligate dimer with Elongin B (13). This results in a six member complex to which an A3 and ARIH2 or an E2 associates to carry out initial monoubiquitination and polyubiqitination, respectively (16). Vif requires CBF-β not directly for A3-mediated ubiquitination, but for thermodynamic stability in cells, which also facilitates assembly with the CRL5 E3 ligase

83 complex (17-19). However, counteraction of APOBEC3 by Vif is not complete and footprints of
84 A3 induced mutations can be found in at least 30% of integrated proviral genomes within 6
85 weeks of infection (20-25). At this early stage of infection the viruses are categorized as
86 transmitted/founder (T/F) viruses (26). Since the Vifs of T/F viruses have not been previously
87 characterized for their ability to suppress A3-mediated restriction, the mechanism behind
88 accumulation of this high number of G→A mutations is not understood.

89 Although there are five human A3 enzymes that can restrict HIV-1, due to the *A3* genes
90 being highly polymorphic, humans usually do not express five *A3* genes that result in enzymes
91 able to restrict HIV (27). The least polymorphic A3 enzymes that have the highest probability to
92 be active against HIV-1 and co-expressed are A3G and A3F (28, 29). Importantly, A3G and A3F
93 form a hetero-oligomer that enhances HIV-1 restriction in the absence of Vif and in the presence
94 of Vif enables the A3F in the hetero-oligomer to become partially resistant to Vif-mediated
95 degradation by a yet-to-be determined mechanism (30, 31). Originally, alanine scanning
96 mutagenesis was used to determine that A3G and A3F interacted with Vif using distinct domains
97 present in the N-terminal and C-terminal domains, respectively (32-35). However, another study
98 using single nucleotide changes based on species specific amino acid differences in A3F
99 determined that the equivalent amino acid at position 128 in the A3G N-terminal domain (NTD)
100 important for Vif-mediated degradation was also important for A3F mediated degradation (36).

101 Although cryo-EM structures of Vif/CBF-β/ElonginB/ElonginC (VCBC) have been
102 determined for A3G and A3H Haplotype II, there is no structural information for how full length
103 A3F interacts with Vif, thus requiring a dependence on mutagenesis studies to be maintained
104 (37-40). A cryo-EM of the A3F C-terminal domain (CTD) with Vif/CBF-β determined that the
105 Vif and CBF-β interface forms a wedge in which the A3F CTD interacts with both proteins (41).

106 The absence of a structure with full length A3F interacting with Vif has hindered our
107 understanding on how the A3F/A3G hetero-oligomer results in partial resistance of A3F to Vif-
108 mediated degradation.

109 In this study, we examined both the mechanism by which A3F resists Vif-mediated
110 degradation in the presence of A3G and if this occurs across a panel of HIV-1 T/F viruses. We
111 identified that A3F interacts with A3G through its NTD and confirmed that the NTD of A3F is
112 required for Vif-mediated degradation, suggesting an A3G-induced protection mechanism from
113 ubiquitination. We determined that his occurred not only with HIV-1_{LAI}, but also all nine
114 different HIV-1 T/F viruses from Subtypes B and C. There were differences in the capability of
115 T/F Vifs to induce degradation of A3G alone, A3F alone, and the A3F/A3G hetero-oligomer
116 despite previously identified interaction domains being conserved. Rather, we determined that
117 regions adjacent to these conserved domains determined differences in HIV-1 T/F Vif-induced
118 degradation, particularly amino acids at positions 155 and 177. Altogether, our data redefine the
119 Vif interaction domain for A3F and for the first time characterize the Vif-mediated degradation
120 of A3G and A3F from HIV-1 T/F viruses.

121 Results

122 A3G protects A3F from HIV-1_{LAI} Vif-mediated degradation

123 A3G and A3F interact through a protein-protein interaction in the absence of an RNA
124 intermediate and this results in partial protection of A3F from Vif-mediated degradation,
125 however the mechanism is not known (30, 31). We studied the A3F/A3G hetero-oligomer using
126 a transfection-based system and a plasmid with two MCS so that each cell that expresses A3F,
127 will also express A3G. The A3F and A3G are uniquely tagged with V5 and HA, respectively, so

128 that they can be identified by immunoblotting. While this precludes comparison between A3G
129 and A3F, we can compare changes among each A3 when it is expressed alone or together to
130 interpret effects of the co-expression.

131 Samples from HIV-1_{LAI} producer cells transfected with A3F-V5, A3G-HA, or A3F-
132 V5/A3G-HA were immunoblotted to detect steady state protein levels in cell lysates (Fig 1A).
133 Previous findings using VSV-G pseudotyped virus were confirmed with a full-length molecular
134 clone of HIV-1_{LAI}. That Vif is responsible for this degradation is demonstrated by the HIV-1_{LAI}
135 SLQ^M that has the Vif SLQ motif needed to interact with Elongin C mutated to AAA (Fig 1A).
136 The HIV-1_{LAI} SLQ^M condition represents the total possible amount of steady state A3 levels in
137 cells (Fig 1A, Cell). This molecular clone expresses Vif, but it cannot form a CRL5 E3 ubiquitin
138 ligase complex. The data demonstrated that Vif-induced degradation by HIV-1_{LAI} of A3F occurs
139 when it is expressed alone (by comparison to HIV-1_{LAI} SLQ^M), but when it is co-expressed with
140 A3G, the A3F is more resistant to Vif-mediated degradation (Fig 1A, Cell).

141 The differences in the levels of A3F when co-expressed with A3G compared to when
142 expressed alone was also apparent in HIV-1_{LAI} virions. The additional A3F in cells in the
143 A3F/A3G condition resulted in increased A3F encapsidation into virions (Fig 1A, Virus).
144 However, the amount of A3G encapsidated in virions was similar in the absence or presence of
145 A3F (Fig 1A, Virus). Altogether, these data demonstrate that the increased steady state level of
146 A3F in cell lysates where A3G is also present results in increased encapsidation of A3F and is
147 due to protection from Vif-mediated degradation.
148

149 ## A3F interacts with A3G through the N-terminal domain

150 Since the A3F/A3G hetero-oligomer results in protection of A3F from Vif-mediated
151 degradation, but not A3G, we hypothesized that the A3F/A3G interface occludes the residues of
152 A3F that interact with Vif. To determine where A3F and A3G interacted and if this overlapped
153 with the A3F and Vif interface, we used domain constructs of A3F and A3G. A3F and A3G are
154 double zinc deaminase domain (ZDD) enzymes and the two ZDD domains can be stably
155 expressed independently since they are connected by a linker region (42). We used co-IP
156 determine if full length A3G-HA or A3F-HA interacted with Flag tagged constructs of the NTD
157 or CTD of A3F or A3G, respectively. The A3G-HA resulted in strong immunoprecipitation of
158 full length A3F and the A3F NTD, but not the A3F CTD (Fig 1B). These data demonstrated that
159 the A3F NTD interacts with A3G. Similarly, to identify the region of A3G that interacts with
160 A3F we used A3F-HA and A3G full length, NTD, and CTD -Flag constructs. A3F-HA resulted
161 in immunoprecipitation of full length A3G and primarily the A3G NTD, but also a lesser amount
162 of the A3G CTD (Fig 1C). These data support a model in which the A3F NTD is primarily
163 interacting with the A3G NTD. While A3G NTD has been shown to interact with Vif, current
164 structural and mutation data with A3F support that the CTD interacts with Vif (33, 41). As a
165 result, these data do not fully explain how A3G can protect A3F from Vif-mediated degradation.
166

167 ## A3F NTD is a determinant in Vif-mediated degradation

168 Although previous structural and biochemical studies have reported that the CTD of A3F
169 interacts with Vif and CBF-β, these data resulted from alanine scanning mutagenesis or Cryo-
170 EM of only the A3F CTD (33, 41). However, even the original study showed that an A3F NTD-
171 A3G CTD chimera interacted with Vif through the A3F NTD and structural models show that

172 the A3F NTD may interact with Vif α1 helix (33, 43). In addition, a single point mutation at A3F
173 amino acid 128, the equivalent amino acid that is a major determinant in the A3G and Vif
174 interaction, can disrupt Vif-mediated degradation of A3F (36). Collectively, these data suggest a
175 previously unidentified key determinant in the A3F NTD for Vif-mediated degradation. As a
176 result, the A3F NTD-A3G NTD interaction may result in occlusion of the A3F residues needed
177 for Vif to efficiently induce A3F degradation, resulting in partial resistance.

178 To confirm and extend past studies, we used the A3F R128T mutant that showed
179 increased restriction compared to A3F of HIV-1 T/F CH077 (36). We compared the HIV-1_{LAI}
180 and HIV-1 T/F CH077 Vif-mediated degradation of A3F and A3F R128T (Fig 2). We measured
181 the steady state levels of A3F and A3F R128T in producer cells of HIV-1_{LAI}, HIV-1_{LAI} SLQ^M,
182 HIV-1 T/F CH077, and HIV-1 T/F CH077 -Vif. For both HIV-1_{LAI} and HIV-1 T/F CH077 the
183 data showed that A3F R128T is more resistant to Vif-mediated degradation than A3F (Fig 2A).
184 That Vif is responsible for the lowered steady state levels of the A3F is demonstrated by the LAI
185 SLQ^M and TF077 -Vif producer cells that do not affect the A3F or A3F R128T steady state
186 levels in cells (Fig 2A).

187 We also conducted an experiment with a Vif expression plasmid and transfected
188 increasing amounts into cells with a constant amount of A3F or A3F R128T. With increasing
189 amounts of Vif transfected, there was increased degradation of A3F and A3F R128T, however at
190 maximum Vif amounts, the A3F remaining was only 14% but for A3F R128T it was 60% (Fig
191 2B). At the lowest Vif transfection condition, the A3F R128T was almost completely resistant to
192 Vif-mediated degradation, but for the A3F, there was a 2-fold decrease in the steady state protein
193 level (Fig 2B). Thus, the A3F R128T mutant is more resistant to Vif-mediated degradation than
194 A3F. Taken together this data demonstrate that the A3F NTD is important for Vif-mediated

195 degradation of A3F and amino acid 128 is a key residue. As a result, the A3G likely occludes
196 this region of A3F, making the Vif-mediated degradation less efficient.

197 A3G partially protects A3F from HIV-1 T/F Vif-mediated 198 degradation

199 To determine if the co-expression of A3F and A3G resulted in partial protection of A3F
200 from Vif expressed from primary isolates, we tested nine different HIV-1 T/F viruses from
201 Subtype B (CH058, CH470, CH040, CH077, Thro) and Subtype C (CH236, CH850, CH569)
202 alongside HIV-1_{LAI}. Analysis of amino acid sequences from HIV-1 T/F Vifs revealed on average
203 12% variation relative to Vif of HIV-1_{LAI} (Fig 3A). The maximum variation was 19% for TF236
204 and the minimum variation was 7% for T/F Thro (Fig 3A). Further inspection of the sequences
205 revealed that the amino acid sequence of the domains reported to be relevant for A3-Vif
206 interactions were conserved and only intervening regions contained the variable amino acids (Fig
207 3B). Thus, we hypothesized that all the T/F Vifs of Subtype B or Subtype C would have similar
208 degradation profiles for A3G, A3F and A3F/A3G when compared to LAI Vif.

209 We selected three HIV-1 T/F molecular clones to study in more depth using single-cycle
210 infectivity assays. The HIV-1 T/F CH040 was used alongside HIV-1_{LAI} to represent Subtype B
211 viruses. The HIV-1 T/F CH850 and CH569 were used to represent Subtype C viruses. We
212 transfected either 25 or 50 ng of plasmids expressing the A3G alone, A3F alone, or A3F/A3G
213 together with the full length molecular clones and determined the relative infectivity in
214 comparison to a no A3 transfection and detected the A3s in producer cells and virions by
215 immunoblotting (Fig 4). The HIV-1_{LAI} SLQ^M was used for comparison in each experiment to
216 determine the amount of A3 enzymes in producer cells and viruses in the absence of Vif-

217 mediated degradation and as an experimental control for maximum A3 restriction (Fig 4 and Fig
218 S1).

219 Although we observed protection of A3F by A3G in the presence of HIV-1_{LAI} by
220 immunoblotting (Figs 1A and 4A), the co-expressed A3F and A3G were not able to restrict HIV-
221 1_{LAI} more than A3G alone, similar to what was reported previously (Fig 4B) (31). The A3G
222 remaining in the cells when alone or co-expressed with A3F was encapsidated (Fig 4A, Virus).
223 This was in contrast to A3F that was not detectable in virions by immunoblotting when
224 expressed alone, but was able to be detected in virions when co-expressed with A3G (Figs 1A
225 and 4A, Virus). However, when determining the infectivity, we observed that HIV-1_{LAI} was
226 restricted similarly when A3G was expressed alone and when expressed with A3F (Fig 4B).
227 Mohammadzadeh *et al*., found similar results for infectivity, but also determined that there was
228 an effect of the A3F/A3G hetero-oligomer upon examining the mutations in proviral sequences
229 (31). The HIV-1_{LAI} was sensitive to restriction when A3G was expressed, despite the presence of
230 Vif and at both 25 and 50 ng transfection conditions. HIV-1_{LAI} was not sensitive to A3F-
231 mediated restriction, consistent with previously reported lower activity of A3F and the increased
232 sensitivity to Vif-mediated degradation (Fig 4A-B) (29, 31). However, the HIV-1 T/F viruses
233 showed different infectivity results from HIV-1_{LAI}, although the immunoblots were similar.

234 Specifically, immunoblotting of producer cell and virus lysates from Subtype B HIV-1
235 T/F CH040 single-cycle infectivity experiments showed modest A3G degradation when alone or
236 co-expressed with A3F and efficient A3F degradation when alone, but not when co-expressed
237 with A3G (Fig 4C, Cell). The A3s that were observed in the cell lysates (A3G alone, A3G co-
238 expressed with A3F, and A3F co-expressed with A3G) were encapsidated (Fig 4C). Despite
239 there being a significant protection of A3F from Vif-mediated degradation and encapsidation of

240 A3F in the presence of A3G, the infectivity data showed no effect of A3G alone, A3F alone, or
241 A3F/A3G on T/F CH040 when only 25 ng of the A3s was transfected (Fig 4C-D). When the
242 transfection level of the A3s was doubled, we observed A3G, but not A3F restriction when both
243 were expressed alone the effect of A3F/A3G co-expression was similar to A3G alone (Fig 4D).
244 The HIV-1 Subtype C T/F viruses CH850 and CH569 showed different infectivity results
245 from the Subtype B viruses. Interestingly, the immunoblots for both HIV-1 T/F CH850 and
246 CH569 were similar to those of the Subtype B viruses and showed modest A3G degradation
247 when alone or co-expressed with A3F, efficient degradation of A3F when expressed alone, and
248 protection of A3F from Vif-mediated degradation when co-expressed with A3G (Fig 4E, G). For
249 HIV-1 T/F CH850, the infectivity was not affected by expression of A3G alone, A3F alone or
250 A3F/A3G at 25 ng plasmid transfection. However, at the 50 ng plasmid transfection we observed
251 no difference in the sensitivity to A3G or A3F alone, but there was ~2-fold more sensitivity to
252 A3F/A3G compared to A3G alone, resulting in only ~30% remaining infectivity (Fig 4F). There
253 was even more of an effect of co-expression of A3F/A3G for HIV-1 T/F CH569 where we
254 observed ~2-fold more reduction in infectivity for A3F/A3G compared to A3G alone at both the
255 25 and 50 ng plasmid transfections with only ~20% infectivity remaining at the higher A3F/A3G
256 transfection amount (Fig 4H). These effects are noteworthy considering that Vif expression is
257 occurring from these molecular clones.
258 Overall, we observed similar results for other Subtype B and C HIV-1 molecular clones
259 (S1 Fig). The Subtype B molecular clones were more sensitive to restriction by A3G when
260 expressed alone and showed no difference from A3G alone for the restriction in the A3G/A3F
261 condition (S1 Fig). The Subtype B molecular clones also showed a large variability in sensitivity
262 to A3G and A3F/A3G, with infectivity ranging from 15-54% (S1 Fig). The Subtype C molecular

263 clones were less sensitive to restriction by A3G when expressed alone, but showed an
264 approximately 2-fold reduction in infectivity in the presence of A3F/A3G in comparison to A3G
265 alone (S1 Fig). None of the molecular clones were sensitive to restriction by A3F when it was
266 expressed alone (S1 Fig).
267

268 HIV-1 T/F Subtype C specific differences in A3G-mediated
269 degradation

270 Despite clear trends emerging from the infectivity data and corresponding immunoblots,
271 we wanted to conduct a more quantitative assay to characterize the potential differences in the
272 Vif-mediated degradation of Subtype B and Subtype C T/F virus Vifs. To this end, we cloned the
273 *vif* from HIV-1_{LAI} and the T/F viruses CH040, CH850, and CH569. We used these clones for A3
274 degradation assays using co-transfection of a constant amount of A3G, A3F or A3F/A3G
275 expression plasmid and increasing amounts of Vif expression plasmid. For the Subtype B Vifs
276 from HIV-1_{LAI} and T/F CH040, there was less A3G remaining in the A3F/A3G condition in
277 comparison to Subtype C virus Vifs (Fig 5A, C, E, G and Table 1, 25 ng). Specifically, for T/F
278 CH040 there was 2-fold to 3-fold less A3G in the A3F/A3G condition when compared to CH850
279 and CH569, respectively (Fig 5C, E, G and Table 1, 25 ng Vif plasmid transfected). This
280 suggests that HIV-1 Subtype B Vifs are more efficient than Subtype C viruses in causing
281 degradation of A3G when it is co-expressed with A3F. There was no consistent subtype
282 differences in the ability of Vif to induce degradation of A3G when expressed alone.
283 An additional difference was that for HIV-1 Subtype B Vifs more A3F remained during
284 A3F/A3G co-expression compared to Subtype C virus Vifs (Fig 5B, D, F, H and Table 2).
285 Specifically, for T/F CH040 there was 2-fold more A3F in the A3F/A3G condition than both

286 CH850 and CH569 (Fig 5D and Table 1, 25 ng Vif plasmid transfected). Higher transfection
287 amounts of the Vif plasmid resulted in equivalent amounts of degradation due to saturation of
288 experimental system with Vif (Fig 5D and Table 1). These data suggest that Subtype C virus
289 Vifs are more active in causing degradation of A3F in the A3F/A3G hetero-oligomer compared
290 to Subtype B virus Vifs. However, for T/F CH850 and CH569 there was still some protection of
291 A3F within the A3F/A3G hetero-oligomer, this was approximately 2-fold less that what was
292 observed with HIV-1_{LAI} and T/F CH040. Interestingly, the Subtype C virus Vifs were not
293 detectable on the blots and were presumably degraded with the A3, in contrast to the Subtype B
294 Vifs that could be detected by immunoblotting (Fig 5). Altogether, these data suggest that the
295 HIV-1 T/F Subtype C viruses are more sensitive to the A3F/A3G hetero-oligomer than HIV-1
296 T/F Subtype B because the Vifs are less able to induce degradation of A3G (Fig 5A, C, E, G).
297

298 Amino acid determinants for Vif-mediated degradation occur
299 outside of conserved domains

300 The Vif domains for interaction with CBF-β, Elongin C and Cullin 5 are well conserved
301 since deviation from these motifs would disrupt function. Nonetheless, we examined the amino
302 acid alignment of the HIV-1 T/F Vifs to determine if we could identify any amino acids in
303 Subtype C in comparison to Subtype B viruses that account for differential abilities of the Vifs to
304 induce A3 degradation (Fig 3B). All analyzed Subtype C viruses, but none of the Subtype B
305 viruses had a Leucine at position 8 that is near the DRMR A3F/A3G interaction domain, a
306 Histidine at position 83 and Leucine at position 91 near the CBF-β interaction domain, and a
307 Methionine and Histidine at 110-111 near the CBF-β and Zn^{2+} interaction domains (Fig 3B).

308 While all these amino acids likely contribute individually or collectively to the
309 differences we observed with infectivity and A3-induced degradation, we focused on CH569
310 since it had a unique profile for infectivity (Fig 4). The CH569 was most sensitive to the
311 A3F/A3G co-expression and this appeared to be due to a lesser ability to induce degradation of
312 A3G, in addition to an inability to induce full degradation of A3F in the A3F/A3G hetero-
313 oligomer (Fig 4H and Fig 5G-H). We observed that CH569 Vif had two unique amino acids
314 from all other Subtype B and Subtype C Vifs that we tested (Fig 3B). We mutated these amino
315 acids to become more like the other T/F Vifs and LAI Vif, resulting in CH569-Q158K and
316 CH569-H177P Vifs.
317 We used these CH569 mutant Vifs in an A3 degradation assay. When A3F was co-
318 expressed with A3G, ~2-fold more A3F was remaining for both CH569 Vif mutants compared to
319 wild type CH569 Vif suggesting these amino acids are required for efficient degradation of A3F
320 in the A3F/A3G hetero-oligomer (Fig 5G-L and Table 2, 25 and 50 ng Vif plasmid transfected).
321 For CH569-Q158K there was also less degradation of A3F alone (Fig 5G-L and Table 2, 25 and
322 50 ng Vif plasmid transfected). Similarly, the CH569-H177P compared to wild type CH569
323 resulted in less degradation of A3F when expressed alone and within the hetero-oligomer (Fig
324 5G-H, K-L and Table 2, 25 ng Vif plasmid transfected). These mutations were predicted to make
325 CH569 more Subtype B-like and the results align well with our HIV-1 Subtype B data where
326 more A3F was remaining in the A3F/A3G expression condition than Subtype C viruses (Fig 5
327 and Table 2, 25 ng Vif plasmid transfected).
328 Interestingly, the CH569 Vif mutants had a different effect on Vif-mediated degradation
329 of A3G alone and A3G in the A3F/A3G condition. While the CH569-H177P mutant had no
330 effect on A3G degradation when expressed alone, the CH569-Q158K mutant was ~6-10 fold

331 more efficient at Vif-mediated degradation of A3G (Fig 5 and Table 1, 25 and 50 ng Vif plasmid
332 transfected). In the A3F/A3G condition, both the CH569 -H177P and -Q158K mutants were ~2-
333 3-fold more efficient at inducing degradation of A3G and more similar to Vif-mediated
334 degradation observed for Subtype B viruses, as would be predicted by the amino acid
335 substitutions (Fig 5 and Table 1, 25 and 50 ng Vif plasmid transfected).
336 Overall, these data suggest that there are still unidentified regions of Vif that are
337 determinants in A3-mediated degradation. This is especially important for understanding the
338 A3F and A3F/A3G interactions with Vif since there is no structural information for full length
339 A3F in complex with Vif.
340

341 Discussion

342 A3 restriction factors are able to induce mutations in HIV-1 proviral DNA despite Vif-
343 mediated degradation. Near full-length sequencing of HIV-1 proviral DNA within the acute
344 infection period has shown that ~95% of proviral DNA becomes inactivated within the first 6
345 weeks of infection and at least 30% of those proviruses have A3-induced G→A mutations,
346 particularly causing stop codons that result in viral inactivation (20, 44). While this initially
347 appeared at odds with a functional Vif protein, A3F and A3G have been shown to hetero-
348 oligomerize and co-encapsidate in order to partially resist Vif-mediated degradation enabling
349 their activity to tip the balance towards viral inactivation (30, 31, 45). We have previously shown
350 that in the presence of Vif and antiretrovirals, A3F/A3G hetero-oligomerization results in partial
351 protection of A3F from Vif-mediated degradation, increased proviral mutations from A3F, and
352 greatly decreased viral fitness compared to the absence of A3s (31). However, how A3F and
353 A3G interacted and if these identified hetero-oligomer features occurred in the presence of HIV-

354 1 T/F Vifs was not known. Here, we determined that the A3F NTD interacts with A3G,
355 confirmed and extended data that suggested the A3F NTD is a determinant in Vif-mediated
356 degradation, determined that multiple HIV-1 T/F viruses lose the ability to fully induce
357 degradation of A3F when it hetero-oligomerizes with A3G, and identified new determinants in
358 Vif-mediated degradation outside of the previously identified domains.

359 The co-IP data demonstrated that A3F the NTD interacted with A3G. An additional
360 consideration in this interaction is the stoichiometry and RNA binding. Ara *et al*. determined that
361 three molecules of A3F interacted with one molecule of A3G (30). However, the orientation of
362 the A3F interacting domains for homo-oligomerization is not known, making it difficult to model
363 the A3F/A3G interaction and how the interaction is able to protect A3F from Vif-mediated
364 degradation. That the NTD of A3F is involved in Vif-mediated degradation and the interaction
365 with A3G suggests that A3G occludes the Vif interaction site, however, it does not explain why
366 other A3F subunits of the hetero-oligomer are also protected from Vif-mediated degradation.
367 One explanation is that both A3G hetero- and A3F homo- oligomerization block the Vif
368 interaction site. Alternatively, since the A3F protection from Vif-mediated degradation is only
369 partial, this could mean that only the A3F interacting with A3G is protected from Vif mediated
370 degradation, and other A3F molecules in the hetero-oligomer are not. Additionally, A3G may
371 also be protected from Vif-mediated degradation when interacting with A3F since the A3G NTD
372 is the Vif interaction domain (13). We may not observe A3G protection from Vif-mediated
373 degradation when interacting with A3F in bulk cell lysate studies because the stoichiometry of
374 the hetero-oligomer involves only one A3G to three A3F (30). Notably, multiple structural
375 studies have demonstrated that Vif interacts with a monomer of A3G and an RNA molecule (37-

376 39). How the RNA molecule associates with the A3F/A3G hetero-oligomer and if A3F also
377 interacts with Vif and RNA remains to be determined.

378 The A3F/A3G hetero-oligomer may affect Vif-mediated ubiquitination. Studies that
379 determined where the CRL5 E3 ligase polyubiquitinates lysines on A3G and A3F found different
380 results. Iwatani *et al*. determined that A3G was polyubiquitinated on four key residues and these
381 could be mutated to block Vif-mediated ubiquitination (46). However, Albin *et al*. determined
382 that although A3G was partially resistant to Vif-mediated degradation when the four key
383 residues identified by Iwatani *et al*. were mutated, it did not result in complete resistance to Vif
384 (46, 47). These results and that A3F was found to be polyubiquitinated throughout the protein
385 and modification of specific lysines could not block Vif-mediated degradation of A3F resulted in
386 the conclusion that ubiquitination of A3s by the CRL5 E3 ligase is relatively stochastic (47). As
387 a result, we hypothesize an all or nothing phenomenon where those A3F molecules interacting
388 with A3G are not ubiquitinated due to not directly interacting with Vif rather than a hypothesis
389 of less efficient ubiquitination of A3F resulting in partial protection of A3F from Vif-mediated
390 degradation.

391 Combined restriction of HIV-1 from A3F and A3G in the presence of Vif has resulted in
392 variable conclusions. An early study found that in the absence of Vif, co-expressed A3G and
393 A3F caused an increase in HIV-1 proviral DNA mutations compared to when each was
394 expressed alone (48). However, effect of co-expression of A3F and A3G on infectivity was only
395 additive (48). Although in the absence of Vif Ara *et al*. found that there was a synergistic effect
396 of A3F and A3G co-expression on HIV-1 proviral mutation rate and restriction, in the presence
397 of Vif Mohammadzadeh *et al*. observed that there was no effect on either of these variables (30,
398 31). Rather, the effects observed by Mohammadzadeh *et al*. were that the proviral mutation type

399 became more diversified and that the viruses were less fit under selective conditions, such as
400 antiretroviral treatment (31). These studies all used HIV-1 Subtype B viruses and our data are in
401 agreement with these studies showing that despite partial protection of A3F from Vif-mediated
402 degradation, in a single-cycle infectivity assay, there is no effect on HIV-1 infectivity above that
403 of A3G alone. There are two hypotheses for these results with HIV-1 Subtype B viruses in our
404 study. This could be due to the lack of a selective pressure that would reveal defects in fitness or
405 that more replication cycles are needed to see a pronounced effect in the presence of Vif. These
406 hypotheses are not mutually exclusive. Mohammadzadeh *et al.* supports the former hypothesis
407 (31). The latter hypothesis is supported by mouse studies. Krisko *et al*. used a BLT humanized
408 mouse model and concluded that for consistent HIV-1 restriction the combined activity of A3F
409 and A3G was required (49). However, Sato *et al*. that utilized a NOG-hCD34 mouse humanized
410 mouse model found that mutations in HIV-1 proviral DNA were caused by deamination activity
411 of either A3G or A3F suggesting that A3F and A3G act individually, but still concluding that
412 they can restrict HIV-1 in the presence of Vif (50).

413 Surprisingly, there was a consistent and different observation when A3F and A3G co-
414 expression occurred during infection with HIV-1 T/F Subtype C viruses. The four HIV-1 T/F
415 Subtype C viruses used in this study all had a 2-fold decrease in infectivity during A3F/A3G co-
416 expression compared to A3G alone (50 ng A3 plasmid transfection). When compared to HIV-1
417 T/F Subtype B viruses, this did not result from only a difference in the level of A3F protection
418 from Vif-mediated degradation, but also a lesser ability to induce degradation of A3G when
419 expressed alone and within the A3F/A3G hetero-oligomer. However, when A3G was expressed
420 alone, the HIV-1 T/F Subtype B and Subtype C viruses showed a large diversity in the A3G-
421 mediated restriction with Subtype B viruses on average being more sensitive than Subtype C

422 viruses to A3G-medated restriction. However, during A3F/A3G co-expression the HIV-1 T/F
423 Subtype C viruses were more sensitive to restriction. These data suggest that the additional A3G
424 encapsidated in the presence of A3F for HIV-1 T/F Subtype C viruses, but not Subtype B viruses
425 causes the more efficient restriction. However, since this does not occur when A3G is expressed
426 alone during HIV-1 T/F Subtype C infection, the data support that there is a contribution of
427 restriction from A3F. This may be due to the increased diversity in proviral DNA mutations as
428 identified by Mohammadzadeh *et al.* (31). Since A3F deaminates the 5'TC motif in (-) DNA, it
429 has a greater number of possible codons that this site overlaps with compared to A3G that
430 deaminates 5'CC (underlined C primarily deaminated) and causes mutations primarily at
431 Glycines (70% of total mutations) (51).

432 The variability in the HIV-1 T/F virus sensitivity to A3G-mediated restriction was
433 surprising since the A3-Vif interaction domains are highly conserved. However, outside of these
434 regions Vifs display variability, particularly subtype specific amino acid variability (52-54).
435 Although, HIV-1 Subtype C is the most prevalent subtype globally and accounts for more than
436 40% global infections there are few studies using HIV-1 Subtype C Vif to map Vif-A3
437 interacting regions, in addition to a lack of A3-Vif studies using Vifs from HIV-1 T/F viruses.
438 Our data indicate that Vif amino acids outside the well-defined Vif-A3 interfaces influence the
439 degradation ability. However, the residues we identified as unique to the HIV-1 T/F CH569 Vif
440 were in a loop region not well defined in cryo-EM or structural studies (37-39, 55). Nonetheless,
441 this region is between the Elongin C interaction site and the PPLP motif of Vif that was
442 previously shown to be important for A3-mediated degradation. As a result, additional structure
443 function studies in this region of Vif are warranted.

444 The data presented here reveal additional details on the A3F/A3G interaction,
445 demonstrate that HIV-1 T/F viruses have differential sensitivities to A3G and A3F/A3G
446 restriction, and that HIV-1 T/F Subtype C viruses are most sensitive than Subtype B viruses to
447 the A3F/A3G hetero-oligomer mediated restriction. Structural studies defining how A3G and
448 A3H interact with VCBC have revealed new facets of the A3-Vif interactions, but there remains
449 no structural information with full length A3F or an understanding of how VCBC interacts with
450 the A3F/A3G hetero-oligomer (37-41). Altogether, the data emphasize that the Vif-A3
451 interaction is still not completely defined and additional studies utilizing T/F viruses, especially
452 those of Subtype C origin are warranted.
453

454 Materials and Methods

455 Plasmids and Molecular Clones

456 The expression plasmids pVIVO2 A3G-HA, pVIVO2 A3F-V5 and pVIVO2 A3F-
457 V5/A3G-HA, have been previously described (30). The following reagents were obtained
458 through the NIH HIV Reagent Program, Division of AIDS, NIAID, NIH: Plasmid pcDNA3.1-
459 APOBEC3G-HA Expressing Human APOBEC3G with C-Terminal Triple HA Tag, ARP-9952,
460 contributed by Dr. Warner C. Greene and Human APOBEC3F V5 His Expression Vector, ARP-
461 10100, contributed by Dr. B. Matija Peterlin and Dr. Yong-Hui Zheng. The ARP-10100
462 APOBEC3F plasmid was subcloned in place of A3G in the ARP-9952 vector background. Flag-
463 tagged constructs in pcDNA3.1 for A3F, A3F-NTD, A3F-CTD, A3G, A3G-NTD, and A3G-
464 CTD were provided by Dr. Xiaojiang S. Chen (University of Southern California). The A3F-V5
465 R128 has been previously described (36). The expression plasmid pcDNA3.1- Vif_{LAI} has been

466 previously described (56). The pCG-Vif-AU1 plasmids were generated by PCR amplifying Vif
467 sequences from infectious molecular clones and inserted using XbaI and MluI sites.

468 The infectious molecular clone of HIV-1_{LAI} and the HIV-1_{LAI} SLQ→AAA (SLQ^M) that
469 contains a mutated Vif that cannot interact with Elongin C or induce degradation of A3s has been
470 previously described (57). The infectious molecular clones for the HIV-1 transmitted founder
471 (T/F) viruses were a gift from Dr. Beatrice Hahn (Perelman School of Medicine, University of
472 Pennsylvania) and have been previously described (58-61). The CH077 -Vif construct has two
473 tandem stop codons inserted in *vif* and was previously described (36).

474 Co-immunoprecipitation

475 The 293T cells were seeded in a T75 cm^2 flask (1 x 10^6) and the next day were
476 transfected with plasmid DNA using GeneJuice transfection reagent (EMD Millipore) as per
477 manufacturer's instructions. Following amounts of plasmid DNA were used: pcDNA3.1 A3F-
478 Flag (4 µg), pcDNA3.1 A3F-NTD-Flag (3 µg), pcDNA3.1 A3F-CTD-Flag (2 µg), pcDNA3.1-
479 A3G-HA (1 µg), pcDNA3.1-A3F-HA (4 µg), pcDNA3.1-A3G-Flag (1 µg), pcDNA3.1-A3G-
480 NTD-Flag (2 µg), and pcDNA3.1-A3G-NTD-Flag (2 µg). Empty pcDNA3.1 was used to
481 equalize the amount of transfected DNA. At 48 h post transfection, the cells were washed with
482 PBS and lysed using IP buffer (50 mM Tris-Cl pH 7.4, 1% Nonidet-P40, 10% glycerol, 150 mM
483 NaCl) supplemented with EDTA-free protease inhibitor (Roche) and clarified by centrifugation.
484 Then 400 µg of cell lysate was added to anti-HA magnetic beads (Sigma) in the presence of
485 RNaseA (50 µg/ml; Roche) and incubated for 2 h with gentle rocking at 4°C. The beads were
486 subsequently washed three times with IP buffer, and the immunoprecipitated proteins were
487 eluted with Laemmli buffer and subjected to SDS-PAGE and immunoblotting with anti-Flag
488 antibody (Cat# F1804, Sigma, 1:1,000), anti-HA antibody (Cat # H6908, Sigma, 1:10,000), and

489 anti-α-tubulin antibody (Cat # PA1-20988, Invitrogen, 1:1,000). Secondary detection was
490 performed using Licor IRDye antibodies produced in goat (IRDye 680-labeled anti-rabbit, 1:
491 10,000 Cat # 926-68071 and IRDye 800-labeled anti mouse, 1:10,000 Cat # 926-32210).

492 A3 degradation assay

493 To investigate the ability of Vif expressed from infectious molecular clones to induce
494 degradation of A3F and A3F R128T, 293T cells (1×10^5 per well) in 12 well plates were co-
495 transfected with pVIVO2 A3F-V5 (50, 100, and 200 ng) or pcDNA3.1 A3F R128T (100, 200,
496 and 300ng) expression vectors and 500 ng of infectious molecular clones of HIV-1_{LAI}, HIV-1_{LAI}
497 SLQ^M, HIV-1 T/F CH077, or HIV-1 T/F CH077 -Vif. At 16 h post transfection the media was
498 changed. After 44 h post transfection, cells were washed with PBS and lysed using 2× Laemmli
499 buffer.

500 In order to compare the efficiency of HIV-1_{LAI} Vif in mediating the degradation of A3F
501 and A3F R128T, 293T cells (1×10^5 per well) in 12 well plates were co-transfected with 100 ng
502 pcDNA3.1 A3F-V5 or 200 ng pcDNA3.1 A3F-V5 R128T and an increasing amount of pcDNA3.1
503 Vif_{LAI} (50, 100, 200, or 300 ng). Then, 16 h post transfection the media was changed. At 44 h post
504 transfection, cells were washed with PBS and lysed using 2× Laemmli buffer.

505 To compare efficiency of different Vifs in mediating degradation of A3G-HA, A3F-V5,
506 and co-expressed A3F-V5/A3G-HA, 293T cells (1×10^5 per well) in 12 well plates were co-
507 transfected with 50 ng of pVIVO2 expressing No A3, A3G-HA, A3F-V5, or A3F-V5/A3G-HA
508 and titration of pCG-Vif-AU1 (0, 25, 50, and 100 ng) using GeneJuice (Novagen) transfection
509 reagent according to manufacturer's instructions. To equalize the amount of plasmid DNA
510 transfected, empty pCG vector was used. Then, 16 h post transfection the media was changed. At
511 44 h post transfection, cells were washed with PBS and lysed using 2× Laemmli buffer.

512 Protein from each cell lysate (30 μg) was resolved by SDS-PAGE used for
513 immunoblotting on nitrocellulose membrane. Primary detection was performed using mouse
514 monoclonal anti-HA antibody (Cat# H9658, Sigma, 1:10,000), anti-V5 mouse monoclonal
515 antibody (Cat# V8012, Sigma, 1:1000), rabbit anti-Vif antibody (Cat# 809, NIH HIV Reagent
516 Program, contributed by Dr. Bryan Cullen, 1:1000) and anti-α tubulin antibody (rabbit
517 polyclonal, Cat# PA1-20988, Invitrogen, 1:1000) Secondary detection was performed using
518 Licor IRDye antibodies produced in goat (IRDye 680-labeled anti-rabbit 1:10,000 Cat # 926-
519 68071 and IRDye 800-labeled anti mouse 1:10,000 Cat # 926-32210). For quantification, Image
520 Studio was used to detect the pixel intensity of the experimental and loading control bands. Each
521 sample was normalized to its own loading control before comparison to other lanes.
522

523 ## Single-cycle infectivity assay

524 Single-cycle infectivity assays were carried out using 1×10^5 293T cells per well in a 12
525 well plate. The 293T cells were maintained in DMEM with 10% FBS in the presence of 5% CO_2
526 at 37°C. Transfections used 500 ng of an HIV-1 infectious molecular clone (LAI, LAI SLQ^M,
527 T/F CH058, T/F CH470, T/F CH040, T/F CH077, T/F Thro, T/F CH236, T/F CH264, T/F
528 CH850, or T/F CH569) and 25 or 50 ng of pVIVO2 containing No A3, A3G-HA, A3F-V5, or
529 both A3F-V5 and A3G-HA. The pVIVO2 (Invivogen) has two MCS to enable co-expression of
530 two genes on a single-cell basis. GeneJuice (EMD Millipore) transfection reagent was used
531 according to manufacturer's instructions. At 16 h post transfection the media was changed.
532 Culture supernatants containing the virus were harvested 46 h post transfection, filtered through
533 0.45 μm polyvinylidene difluoride (PVDF) syringe filters and used to infect TZM-bl cells. TZM-
534 bl cells were plated at 1×10^4 cells per well of a 96-well plate and infected with a serial dilution

535 of the virus in the presence of polybrene (8 μg/mL). The TZM-bl cells were maintained in
536 DMEM with 10% FBS in the presence of 5% CO2 at 37°C. Forty-eight hours after infection the
537 cells were washed with PBS and infectivity was measured through colorimetric detection using a
538 β-galactosidase assay reagent and spectrophotometer. Infectivity of each virus was compared by
539 setting the infectivity of the "No A3" condition as 100%.

540 Immunoblotting cell and virus lysates

541 The cells and culture supernatants used for immunoblotting were obtained from the
542 single-cycle infectivity assays. Cells were washed with PBS and lysed with 2x Laemmli buffer.
543 Total protein in the cell lysate (30 μg) was resolved by SDS-PAGE for immunoblotting on a
544 nitrocellulose membrane. A3 encapsidation was determined by concentrating the virus
545 containing supernatant using Retro-X Concentrator (Clontech) following the manufacturer's
546 protocol, resuspending the pellet in 45 μL of Laemmli buffer and resolving 12 μL of the virus
547 concentrate by SDS-PAGE for immunoblotting on a nitrocellulose membrane. HA tagged
548 proteins were detected in cell lysates using mouse monoclonal anti-HA antibody (Cat# H9658,
549 Sigma, 1:10,000). HA tagged proteins were detected in virus lysates using rabbit polyclonal
550 anti-HA antibody (Cat# H6908, Sigma, 1:1,000). The V5 tagged proteins were detected in cell
551 and virus lysates using anti-V5 mouse monoclonal antibody (Cat# V8012, Sigma, 1:1,000).
552 Loading control for cell lysate was detected with anti-α-tubulin (rabbit polyclonal, Cat# PA1-
553 20988, Invitrogen, 1:5,000) and for virus lysate was detected with anti-p24 (mouse monoclonal,
554 Cat #3537, NIH HIV Reagent Program, 1:1,000). Secondary detection was performed using
555 Licor IRDye antibodies produced in goat (IRDye 680-labeled anti-rabbit 1: 10,000 Cat # 926-
556 68071 and IRDye 800-labeled anti mouse 1:10,000 Cat # 926-32210).
557

558 # References

559 1. Uriu K, Kosugi Y, Suzuki N, Ito J, Sato K. Elucidation of the Complicated Scenario of
560 Primate APOBEC3 Gene Evolution. J Virol. 2021;95(12).
561 2. Cheng AZ, Yockteng-Melgar J, Jarvis MC, Malik-Soni N, Borozan I, Carpenter MA, et
562 al. Epstein-Barr virus BORF2 inhibits cellular APOBEC3B to preserve viral genome integrity.
563 Nat Microbiol. 2019;4(1):78-88.
564 3. Renner TM, Belanger K, Goodwin LR, Campbell M, Langlois MA. Characterization of
565 molecular attributes that influence LINE-1 restriction by all seven human APOBEC3 proteins.
566 Virology. 2018;520:127-36.
567 4. Gaba A, Flath B, Chelico L. Examination of the APOBEC3 Barrier to Cross Species
568 Transmission of Primate Lentiviruses. Viruses. 2021;13(6).
569 5. Richardson SR, Narvaiza I, Planegger RA, Weitzman MD, Moran JV. APOBEC3A
570 deaminates transiently exposed single-strand DNA during LINE-1 retrotransposition. Elife.
571 2014;3:e02008.
572 6. Pollpeter D, Parsons M, Sobala AE, Coxhead S, Lang RD, Bruns AM, et al. Deep
573 sequencing of HIV-1 reverse transcripts reveals the multifaceted antiviral functions of
574 APOBEC3G. Nat Microbiol. 2018;3(2):220-33.
575 7. Wittkopp CJ, Adolph MB, Wu LI, Chelico L, Emerman M. A Single Nucleotide
576 Polymorphism in Human APOBEC3C Enhances Restriction of Lentiviruses. PLoS Pathog.
577 2016;12(10):e1005865.
578 8. Dang Y, Wang X, Esselman WJ, Zheng YH. Identification of APOBEC3DE as another
579 antiretroviral factor from the human APOBEC family. J Virol. 2006;80(21):10522-33.
580 9. Wiegand HL, Doehle BP, Bogerd HP, Cullen BR. A second human antiretroviral factor,
581 APOBEC3F, is suppressed by the HIV-1 and HIV-2 Vif proteins. EMBO J. 2004;23(12):2451-8.
582 10. Sheehy AM, Gaddis NC, Choi JD, Malim MH. Isolation of a human gene that inhibits
583 HIV-1 infection and is suppressed by the viral Vif protein. Nature. 2002;418(6898):646-50.
584 11. OhAinle M, Kerns JA, Li MM, Malik HS, Emerman M. Antiretroelement activity of
585 APOBEC3H was lost twice in recent human evolution. Cell Host Microbe. 2008;4(3):249-59.
586 12. Feng Y, Baig TT, Love RP, Chelico L. Suppression of APOBEC3-mediated restriction of
587 HIV-1 by Vif. Front Microbiol. 2014;5:450.
588 13. Desimmie BA, Delviks-Frankenberrry KA, Burdick RC, Qi D, Izumi T, Pathak VK.
589 Multiple APOBEC3 restriction factors for HIV-1 and one Vif to rule them all. J Mol Biol.
590 2014;426(6):1220-45.
591 14. Apolonia L, Schulz R, Curk T, Rocha P, Swanson CM, Schaller T, et al. Promiscuous
592 RNA binding ensures effective encapsidation of APOBEC3 proteins by HIV-1. PLoS Pathog.
593 2015;11(1):e1004609.
594 15. York A, Kutluay SB, Errando M, Bieniasz PD. The RNA Binding Specificity of Human
595 APOBEC3 Proteins Resembles That of HIV-1 Nucleocapsid. PLoS Pathog.
596 2016;12(8):e1005833.
597 16. Huttenhain R, Xu J, Burton LA, Gordon DE, Hultquist JF, Johnson JR, et al. ARIH2 Is a
598 Vif-Dependent Regulator of CUL5-Mediated APOBEC3G Degradation in HIV Infection. Cell
599 Host Microbe. 2019;26(1):86-99 e7.
600 17. Zhang W, Du J, Evans SL, Yu Y, Yu XF. T-cell differentiation factor CBF-beta regulates
601 HIV-1 Vif-mediated evasion of host restriction. Nature. 2011;481(7381):376-9.
602 18. Jager S, Kim DY, Hultquist JF, Shindo K, LaRue RS, Kwon E, et al. Vif hijacks CBF-
603 beta to degrade APOBEC3G and promote HIV-1 infection. Nature. 2011;481(7381):371-5.

604 19. Zhou X, Evans SL, Han X, Liu Y, Yu XF. Characterization of the interaction of full-
605 length HIV-1 Vif protein with its key regulator CBFbeta and CRL5 E3 ubiquitin ligase
606 components. PLoS One. 2012;7(3):e33495.
607 20. Bruner KM, Murray AJ, Pollack RA, Soliman MG, Laskey SB, Capoferri AA, et al.
608 Defective proviruses rapidly accumulate during acute HIV-1 infection. Nature medicine.
609 2016;22(9):1043-9.
610 21. Piantadosi A, Humes D, Chohan B, McClelland RS, Overbaugh J. Analysis of the
611 percentage of human immunodeficiency virus type 1 sequences that are hypermutated and
612 markers of disease progression in a longitudinal cohort, including one individual with a partially
613 defective Vif. J Virol. 2009;83(16):7805-14.
614 22. Armitage AE, Deforche K, Welch JJ, Van Laethem K, Camacho R, Rambaut A, et al.
615 Possible footprints of APOBEC3F and/or other APOBEC3 deaminases, but not APOBEC3G, on
616 HIV-1 from patients with acute/early and chronic infections. J Virol. 2014;88(21):12882-94.
617 23. Pace C, Keller J, Nolan D, James I, Gaudieri S, Moore C, et al. Population level analysis
618 of human immunodeficiency virus type 1 hypermutation and its relationship with APOBEC3G
619 and vif genetic variation. J Virol. 2006;80(18):9259-69.
620 24. Ooms M, Brayton B, Letko M, Maio SM, Pilcher CD, Hecht FM, et al. HIV-1 Vif
621 adaptation to human APOBEC3H haplotypes. Cell Host Microbe. 2013;14(4):411-21.
622 25. Lian X, Gao C, Sun X, Jiang C, Einkauf KB, Seiger KW, et al. Signatures of immune
623 selection in intact and defective proviruses distinguish HIV-1 elite controllers. Sci Transl Med.
624 2021;13(624):eabl4097.
625 26. Keele BF, Giorgi EE, Salazar-Gonzalez JF, Decker JM, Pham KT, Salazar MG, et al.
626 Identification and characterization of transmitted and early founder virus envelopes in primary
627 HIV-1 infection. Proc Natl Acad Sci U S A. 2008;105(21):7552-7.
628 27. Duggal NK, Fu W, Akey JM, Emerman M. Identification and antiviral activity of
629 common polymorphisms in the APOBEC3 locus in human populations. Virology.
630 2013;443(2):329-37.
631 28. Refsland EW, Stenglein MD, Shindo K, Albin JS, Brown WL, Harris RS. Quantitative
632 profiling of the full APOBEC3 mRNA repertoire in lymphocytes and tissues: implications for
633 HIV-1 restriction. Nucleic Acids Res. 2010;38(13):4274-84.
634 29. Chaipan C, Smith JL, Hu WS, Pathak VK. APOBEC3G restricts HIV-1 to a greater
635 extent than APOBEC3F and APOBEC3DE in human primary CD4+ T cells and macrophages. J
636 Virol. 2013;87(1):444-53.
637 30. Ara A, Love RP, Follack TB, Ahmed KA, Adolph MB, Chelico L. Mechanism of
638 Enhanced HIV Restriction by Virion Coencapsidated Cytidine Deaminases APOBEC3F and
639 APOBEC3G. J Virol. 2017;91(3).
640 31. Mohammadzadeh N, Love RP, Gibson R, Arts EJ, Poon AFY, Chelico L. Role of co-
641 expressed APOBEC3F and APOBEC3G in inducing HIV-1 drug resistance. Heliyon.
642 2019;5(4):e01498.
643 32. Smith JL, Pathak VK. Identification of specific determinants of human APOBEC3F,
644 APOBEC3C, and APOBEC3DE and African green monkey APOBEC3F that interact with HIV-
645 1 Vif. J Virol. 2010;84(24):12599-608.
646 33. Russell RA, Smith J, Barr R, Bhattacharyya D, Pathak VK. Distinct domains within
647 APOBEC3G and APOBEC3F interact with separate regions of human immunodeficiency virus
648 type 1 Vif. J Virol. 2009;83(4):1992-2003.

649 34. Hache G, Liddament MT, Harris RS. The retroviral hypermutation specificity of
650 APOBEC3F and APOBEC3G is governed by the C-terminal DNA cytosine deaminase domain. J
651 Biol Chem. 2005;280(12):10920-4.
652 35. Navarro F, Bollman B, Chen H, Konig R, Yu Q, Chiles K, et al. Complementary function
653 of the two catalytic domains of APOBEC3G. Virology. 2005;333(2):374-86.
654 36. Nchioua R, Kmiec D, Gaba A, Sturzel CM, Follack T, Patrick S, et al. APOBEC3F
655 Constitutes a Barrier to Successful Cross-Species Transmission of Simian Immunodeficiency
656 Virus SIVsmm to Humans. J Virol. 2021;95(17):e0080821.
657 37. Kouno T, Shibata S, Shigematsu M, Hyun J, Kim TG, Matsuo H, et al. Structural insights
658 into RNA bridging between HIV-1 Vif and antiviral factor APOBEC3G. Nat Commun.
659 2023;14(1):4037.
660 38. Li YL, Langley CA, Azumaya CM, Echeverria I, Chesarino NM, Emerman M, et al. The
661 structural basis for HIV-1 Vif antagonism of human APOBEC3G. Nature. 2023;615(7953):728-
662 33.
663 39. Ito F, Alvarez-Cabrera AL, Liu S, Yang H, Shiriaeva A, Zhou ZH, et al. Structural basis
664 for HIV-1 antagonism of host APOBEC3G via Cullin E3 ligase. Sci Adv. 2023;9(1):eade3168.
665 40. Ito F, Alvarez-Cabrera AL, Kim K, Zhou ZH, Chen XS. Structural basis of HIV-1 Vif-
666 mediated E3 ligase targeting of host APOBEC3H. Nat Commun. 2023;14(1):5241.
667 41. Hu Y, Desimmie BA, Nguyen HC, Ziegler SJ, Cheng TC, Chen J, et al. Structural basis
668 of antagonism of human APOBEC3F by HIV-1 Vif. Nat Struct Mol Biol. 2019;26(12):1176-83.
669 42. Yang H, Ito F, Wolfe AD, Li S, Mohammadzadeh N, Love RP, et al. Understanding the
670 structural basis of HIV-1 restriction by the full length double-domain APOBEC3G. Nat
671 Commun. 2020;11(1):632.
672 43. Hu Y, Knecht KM, Shen Q, Xiong Y. Multifaceted HIV-1 Vif interactions with human
673 E3 ubiquitin ligase and APOBEC3s. FEBS J. 2021;288(11):3407-17.
674 44. Li Y, Etemad B, Dele-Oni R, Sharaf R, Gao C, Lichterfeld M, et al. Drug resistance
675 mutations in HIV provirus are associated with defective proviral genomes with hypermutation.
676 AIDS. 2021;35(7):1015-20.
677 45. Desimmie BA, Burdick RC, Izumi T, Doi H, Shao W, Alvord WG, et al. APOBEC3
678 proteins can copackage and comutate HIV-1 genomes. Nucleic Acids Res. 2016;44(16):7848-65.
679 46. Iwatani Y, Chan DS, Liu L, Yoshii H, Shibata J, Yamamoto N, et al. HIV-1 Vif-mediated
680 ubiquitination/degradation of APOBEC3G involves four critical lysine residues in its C-terminal
681 domain. Proc Natl Acad Sci U S A. 2009;106(46):19539-44.
682 47. Albin JS, Anderson JS, Johnson JR, Harjes E, Matsuo H, Krogan NJ, et al. Dispersed
683 sites of HIV Vif-dependent polyubiquitination in the DNA deaminase APOBEC3F. J Mol Biol.
684 2013;425(7):1172-82.
685 48. Liddament MT, Brown WL, Schumacher AJ, Harris RS. APOBEC3F properties and
686 hypermutation preferences indicate activity against HIV-1 in vivo. Curr Biol. 2004;14(15):1385-
687 91.
688 49. Krisko JF, Begum N, Baker CE, Foster JL, Garcia JV. APOBEC3G and APOBEC3F Act
689 in Concert To Extinguish HIV-1 Replication. J Virol. 2016;90(9):4681-95.
690 50. Sato K, Izumi T, Misawa N, Kobayashi T, Yamashita Y, Ohmichi M, et al. Remarkable
691 lethal G-to-A mutations in vif-proficient HIV-1 provirus by individual APOBEC3 proteins in
692 humanized mice. J Virol. 2010;84(18):9546-56.
693 51. Adolph MB, Love RP, Chelico L. Biochemical Basis of APOBEC3 Deoxycytidine
694 Deaminase Activity on Diverse DNA Substrates. ACS Infect Dis. 2018;4(3):224-38.

695 52. Simon V, Zennou V, Murray D, Huang Y, Ho DD, Bieniasz PD. Natural variation in Vif:
696 differential impact on APOBEC3G/3F and a potential role in HIV-1 diversification. PLoS
697 Pathog. 2005;1(1):e6.
698 53. Jacobs GB, Nistal M, Laten A, van Rensburg EJ, Rethwilm A, Preiser W, et al.
699 Molecular analysis of HIV type 1 vif sequences from Cape Town, South Africa. AIDS Res Hum
700 Retroviruses. 2008;24(7):991-4.
701 54. Stephens EB, Singh DK, Pacyniak E, McCormick C. Comparison of Vif sequences from
702 diverse geographical isolates of HIV type 1 and SIV(cpz) identifies substitutions common to
703 subtype C isolates and extensive variation in a proposed nuclear transport inhibition signal.
704 AIDS Res Hum Retroviruses. 2001;17(2):169-77.
705 55. Guo Y, Dong L, Qiu X, Wang Y, Zhang B, Liu H, et al. Structural basis for hijacking
706 CBF-beta and CUL5 E3 ligase complex by HIV-1 Vif. Nature. 2014;505(7482):229-33.
707 56. Baig TT, Feng Y, Chelico L. Determinants of efficient degradation of APOBEC3
708 restriction factors by HIV-1 Vif. J Virol. 2014;88(24):14380-95.
709 57. Ooms M, Letko M, Simon V. The Structural Interface between HIV-1 Vif and Human
710 APOBEC3H. J Virol. 2017;91(5).
711 58. Fenton-May AE, Dibben O, Emmerich T, Ding H, Pfafferott K, Aasa-Chapman MM, et
712 al. Relative resistance of HIV-1 founder viruses to control by interferon-alpha. Retrovirology.
713 2013;10:146.
714 59. Ochsenbauer C, Edmonds TG, Ding H, Keele BF, Decker J, Salazar MG, et al.
715 Generation of transmitted/founder HIV-1 infectious molecular clones and characterization of
716 their replication capacity in CD4 T lymphocytes and monocyte-derived macrophages. J Virol.
717 2012;86(5):2715-28.
718 60. Parrish NF, Gao F, Li H, Giorgi EE, Barbian HJ, Parrish EH, et al. Phenotypic properties
719 of transmitted founder HIV-1. Proc Natl Acad Sci U S A. 2013;110(17):6626-33.
720 61. Wang C, Liu D, Zuo T, Hora B, Cai F, Ding H, et al. Accumulated mutations by 6
721 months of infection collectively render transmitted/founder HIV-1 significantly less fit. J Infect.
722 2020;80(2):210-8.
723 62. Gaba A, Hix MA, Suhail S, Flath B, Boysan B, Williams DR, et al. Divergence in
724 Dimerization and Activity of Primate APOBEC3C. J Mol Biol. 2021;433(24):167306.
725 63. Dereeper A, Guignon V, Blanc G, Audic S, Buffet S, Chevenet F, et al. Phylogeny.fr:
726 robust phylogenetic analysis for the non-specialist. Nucleic Acids Res. 2008;36(Web Server
727 issue):W465-9.
728 64. Russell RA, Pathak VK. Identification of two distinct human immunodeficiency virus
729 type 1 Vif determinants critical for interactions with human APOBEC3G and APOBEC3F. J
730 Virol. 2007;81(15):8201-10.
731 65. Tian C, Yu X, Zhang W, Wang T, Xu R, Yu XF. Differential requirement for conserved
732 tryptophans in human immunodeficiency virus type 1 Vif for the selective suppression of
733 APOBEC3G and APOBEC3F. J Virol. 2006;80(6):3112-5.
734 66. Mehle A, Wilson H, Zhang C, Brazier AJ, McPike M, Pery E, et al. Identification of an
735 APOBEC3G binding site in human immunodeficiency virus type 1 Vif and inhibitors of Vif-
736 APOBEC3G binding. J Virol. 2007;81(23):13235-41.
737 67. He Z, Zhang W, Chen G, Xu R, Yu XF. Characterization of conserved motifs in HIV-1
738 Vif required for APOBEC3G and APOBEC3F interaction. J Mol Biol. 2008;381(4):1000-11.

739 68. Yamashita T, Kamada K, Hatcho K, Adachi A, Nomaguchi M. Identification of amino
740 acid residues in HIV-1 Vif critical for binding and exclusion of APOBEC3G/F. Microbes Infect.
741 2008;10(10-11):1142-9.
742 69. Dang Y, Wang X, Zhou T, York IA, Zheng YH. Identification of a novel WxSLVK motif
743 in the N terminus of human immunodeficiency virus and simian immunodeficiency virus Vif that
744 is critical for APOBEC3G and APOBEC3F neutralization. J Virol. 2009;83(17):8544-52.
745 70. Pery E, Rajendran KS, Brazier AJ, Gabuzda D. Regulation of APOBEC3 proteins by a
746 novel YXXL motif in human immunodeficiency virus type 1 Vif and simian immunodeficiency
747 virus SIVagm Vif. J Virol. 2009;83(5):2374-81.
748 71. Binka M, Ooms M, Steward M, Simon V. The activity spectrum of Vif from multiple
749 HIV-1 subtypes against APOBEC3G, APOBEC3F, and APOBEC3H. J Virol. 2012;86(1):49-59.
750 72. Ooms M, Letko M, Binka M, Simon V. The resistance of human APOBEC3H to HIV-1
751 NL4-3 molecular clone is determined by a single amino acid in Vif. PLoS One.
752 2013;8(2):e57744.
753 73. Wang H, Liu B, Liu X, Li Z, Yu XF, Zhang W. Identification of HIV-1 Vif regions
754 required for CBF-beta interaction and APOBEC3 suppression. PLoS One. 2014;9(5):e95738.
755 74. Mehle A, Strack B, Ancuta P, Zhang C, McPike M, Gabuzda D. Vif overcomes the
756 innate antiviral activity of APOBEC3G by promoting its degradation in the ubiquitin-proteasome
757 pathway. J Biol Chem. 2004;279(9):7792-8.
758 75. Stanley BJ, Ehrlich ES, Short L, Yu Y, Xiao Z, Yu XF, et al. Structural insight into the
759 human immunodeficiency virus Vif SOCS box and its role in human E3 ubiquitin ligase
760 assembly. J Virol. 2008;82(17):8656-63.
761 76. Yu Y, Xiao Z, Ehrlich ES, Yu X, Yu XF. Selective assembly of HIV-1 Vif-Cul5-
762 ElonginB-ElonginC E3 ubiquitin ligase complex through a novel SOCS box and upstream
763 cysteines. Genes Dev. 2004;18(23):2867-72.
764 77. Luo K, Xiao Z, Ehrlich E, Yu Y, Liu B, Zheng S, et al. Primate lentiviral virion
765 infectivity factors are substrate receptors that assemble with cullin 5-E3 ligase through a HCCH
766 motif to suppress APOBEC3G. Proc Natl Acad Sci U S A. 2005;102(32):11444-9.
767 78. Xiao Z, Ehrlich E, Yu Y, Luo K, Wang T, Tian C, et al. Assembly of HIV-1 Vif-Cul5 E3
768 ubiquitin ligase through a novel zinc-binding domain-stabilized hydrophobic interface in Vif.
769 Virology. 2006;349(2):290-9.
770 79. Corpet F. Multiple sequence alignment with hierarchical clustering. Nucleic Acids Res.
771 1988;16(22):10881-90.

772

773 # Acknowledgments

774 We acknowledge Quinlan Carter for technical assistance with this work.

775

776

Figure Legends

Fig. 1. The A3F and A3G interaction results in partial protection of A3F from HIV-1$_{LAI}$ Vif-mediated degradation. (A) HIV-1$_{LAI}$ (LAI) and LAI SLQ mutant (SLQ^{M}) viruses were used to determine the Vif-mediated degradation of A3F and A3G. The SLQ^{M} is SLQ→AAA and prevents Vif from interacting with Elongin C. Immunoblotting with anti-HA and anti-V5 was used to detect A3G and A3F respectively, in cell and virus lysates when each was expressed alone (A3G-HA, A3F-V5) or co-expressed (A3F-V5/A3G-HA). The anti-α-tubulin and anti-p24 were used as loading controls for cell and virus lysates, respectively. **(B)** Cell lysates co-transfected with expression plasmids for A3G-HA and A3F-Flag, A3F NTD-Flag, or A3F CTD-Flag were immunoprecipitated with anti-HA antibody, resolved with SDS-PAGE and transferred to nitrocellulose membrane. Immunoblotting with anti-HA and anti-V5 demonstrated that the A3F NTD interacted with A3G. The anti-α-tubulin was used as loading control for the input. **(C)** Cell lysates co-transfected with expression plasmids for A3F-HA and A3G-Flag, A3G NTD-Flag, or A3G CTD-Flag were immunoprecipitated with anti-HA antibody, resolved with SDS-PAGE and transferred to nitrocellulose membrane. Immunoblotting with anti-HA and anti-V5 demonstrated that predominantly the A3G NTD, but also the A3G CTD interacted with A3F. The anti-α-tubulin was used as loading control for the input.

Fig. 2. The A3F NTD is a determinant for Vif-mediated degradation. (A) Cells were transfected with molecular clones of HIV-1$_{LAI}$, HIV-1$_{LAI}$ SLQ^{M}, HIV-1 T/F CH077, or HIV-1 CH077 -Vif and increasing amounts of A3F-V5 (50, 100, or 200 ng) or A3F-V5 R128T (100, 200, or 300 ng) expression plasmid. Cell lysates were collected at 48 h, resolved by SDS-PAGE, transferred to nitrocellulose membrane, and probed with anti-V5 and anti-α-tubulin antibodies.

800 The α-tubulin served as the loading control. **(B)** Cells were transfected with a constant amount of
801 A3F-V5 (100 ng) or A3F-V5 R128T (200 ng) expression plasmid and increasing amounts of
802 HIV-1_{LAI} Vif expression construct (50, 100, 200, or 300ng). Cell lysates were collected at 48 h,
803 resolved by SDS-PAGE, transferred to nitrocellulose membrane, and probed with anti-V5 and
804 anti-Vif antibodies with α-tubulin serving as loading control. The blot was analyzed to determine
805 the band intensity of the A3 with each normalized to the α-tubulin loading control in the same
806 sample. The values were converted to A3F remaining by normalizing to the 0 ng of transfected
807 Vif_{LAI} condition, which was set to a value of 100%.

808 **Fig. 3. Phylogeny and amino acid alignment of HIV-1 T/F Vifs. (A)** Phylogenetic analysis of
809 Vif amino acid sequences of TF viruses used in this study was done using the web server
810 phylogeny.fr (63). **(B)** Alignment of Vif amino acid sequences from HIV-1_{LAI} and HIV-1 T/F
811 viruses used in this study. HIV-1_{LAI} was used as the consensus Vif sequence (top). Dots indicate
812 exact amino acid identity, amino acids indicate differences, and dashes indicate gaps introduced
813 to optimize the alignment. Red indicates high consensus, blue indicates low consensus, and black
814 is neutral. The symbols in the consensus sequence indicate the following amino acids: != I, V; $
815 =L, M; and #=B, D, E, N, Q, Z where B is D or N and Z is E or Q. Known Vif interaction motifs
816 are indicated and were obtained from (55, 64-78). EloC is Elongin C, Cul5 is Cullin 5, Zn is Zinc
817 binding domain. Alignment was done with MultAlin (79).

818

819 **Fig. 4. HIV-1 T/F viruses have variable infectivity in the presence of A3F, A3G, and**
820 **A3F/A3G.** 293T cells were co-transfected with No A3 (empty vector), A3G-HA (A3G), A3F-V5
821 (A3F) or A3F-V5/ A3G-HA (A3F/A3G) expression plasmid and a molecular clone of **(A-B)**

822 HIV-1_{LAI} **(C-D)** HIV-1 T/F CH040 **(E-F)** HIV-1 T/F CH850 or **(G-H)** HIV-1 T/F CH569. For
823 immunoblots, cell lysates and virus lysates were collected at 48 h resolved by SDS-PAGE and
824 transferred to nitrocellulose membrane for probing with anti-V5 and anti-HA. The HIV-1_{LAI}
825 SLQ^M was used as a no Vif control. The anti-α-tubulin and anti-p24 served as loading control for
826 cell and virus lysate, respectively. For immunoblots, 50 ng of A3 expression plasmid was used.
827 The relative infectivity was determined using relative β-galactosidase activity from infected
828 TZM-bl cells normalized to the No A3 condition. Viruses used to infect TZM-bl cells were
829 produced from cells transfected with 25 or 50 ng of A3 expression plasmid. Error bars represent
830 the error range from two independent experiments.

831 **Fig. 5. Vif-mediated degradation of A3F, A3G, and A3F/A3G differs between HIV-1**
832 **Subtype B and Subtype C viruses.** 293T cells were co-transfected with plasmid expressing
833 either A3G-HA (A3G), A3F-V5 (A3F) or A3F-V5/A3G-HA (A3F/A3G) and increasing amount
834 of Vif-AU1 expression plasmid from HIV-1 **(A-B)** LAI **(C-D)** T/F CH040 **(E-F)** T/F CH850,
835 **(G-H)** T/F CH569, **(I-J)** T/F CH569 Q158K, and **(K-L)** T/F CH569 H177P. Cell lysates were
836 collected at 44 h, resolved by SDS-PAGE and transferred to nitrocellulose membrane for probing
837 with anti-V5, anti-HA and anti-Vif antibody. The anti-α-tubulin was the loading control.

838 # Supporting information

839 **S1 Fig**. **HIV-1 T/F viruses have variable infectivity and Vif function in the presence of A3F,**
840 **A3G, and A3F/A3G.** 293T cells were co-transfected with No A3 (empty vector), A3G-HA
841 (A3G), A3F-V5 (A3F) or A3F-V5/A3G-HA (A3F/A3G) and an HIV-1 infectious molecular
842 clone (labeled on figure). **(A)** The infectivity was determined relative to No A3 being set at
843 100% (hatched line). Error bars represent the error range from two independent experiments.
844 Data was replotted from Fig 5 to compare to other HIV-1 T/F viruses. **(B-G)** For immunoblots,
845 cell lysates and virus lysates were collected at 48 h resolved by SDS-PAGE and transferred to
846 nitrocellulose membrane for probing with anti-V5 and anti-HA. The anti-α-tubulin and anti-p24
847 served as loading control for cell and virus lysate, respectively. The relative infectivity was
848 determined using relative β-galactosidase activity from infected TZM-bl cells normalized to the
849 No A3 condition.
850

851 **Table 1. Relative A3G detected by immunoblotting in the presence of Vif.**

Condition (Vif plasmid transfected)	A3G remaining (%)					
	LAI	CH040	CH850	CH569	CH569 Q158K	CH569 H177P
A3G (25 ng)	0.4	5.9	0.0	4.7	0.4	3.8
A3G (50 ng)	1.0	1.5	0.0	6.6	1.2	2.2
A3G (100 ng)	0.4	0.4	0.0	0.0	0.7	0.8
A3F/A3G (25 ng)	0.0	6.4	13	19	7.5	8.1
A3F/A3G (50 ng)	0.0	0.0	4.9	12	3.8	3.0
A3F/A3G (100 ng)	0.0	0.0	12	9.3	11	2.4

852 The blot was analyzed to determine the band intensity of the A3 with each normalized to the α-
853 tubulin loading control in the same sample. The values were converted to A3G remaining by
854 normalizing to the 0 ng of transfected Vif condition, which was set to a value of 100%. The 0 ng
855 of transfected Vif is shown in Fig 5.

856 **Table 2. Relative A3F detected by immunoblotting in the presence of Vif.**

Condition (Vif plasmid transfected)	A3F Remaining (%)					
	LAI	CH040	CH850	CH569	CH569 Q158K	CH569 H177P
A3F (25 ng)	0.0	17	0.0	0.0	11	41
A3F (50 ng)	0.0	6.1	0.0	0.0	16	12
A3F (100 ng)	0.0	0.0	0.0	0.0	8.1	7.0
A3F/A3G (25 ng)	31	29	12	14	34	30
A3F/A3G (50 ng)	22	14	14	10	31	20
A3F/A3G (100 ng)	12	17	24	10	23	9.3

857 The blot was analyzed to determine the band intensity of the A3 with each normalized to the α-
858 tubulin loading control in the same sample. The values were converted to A3F remaining by
859 normalizing to the 0 ng of transfected Vif condition, which was set to a value of 100%. The 0 ng
860 of transfected Vif is shown in Fig 5.

Fig 1

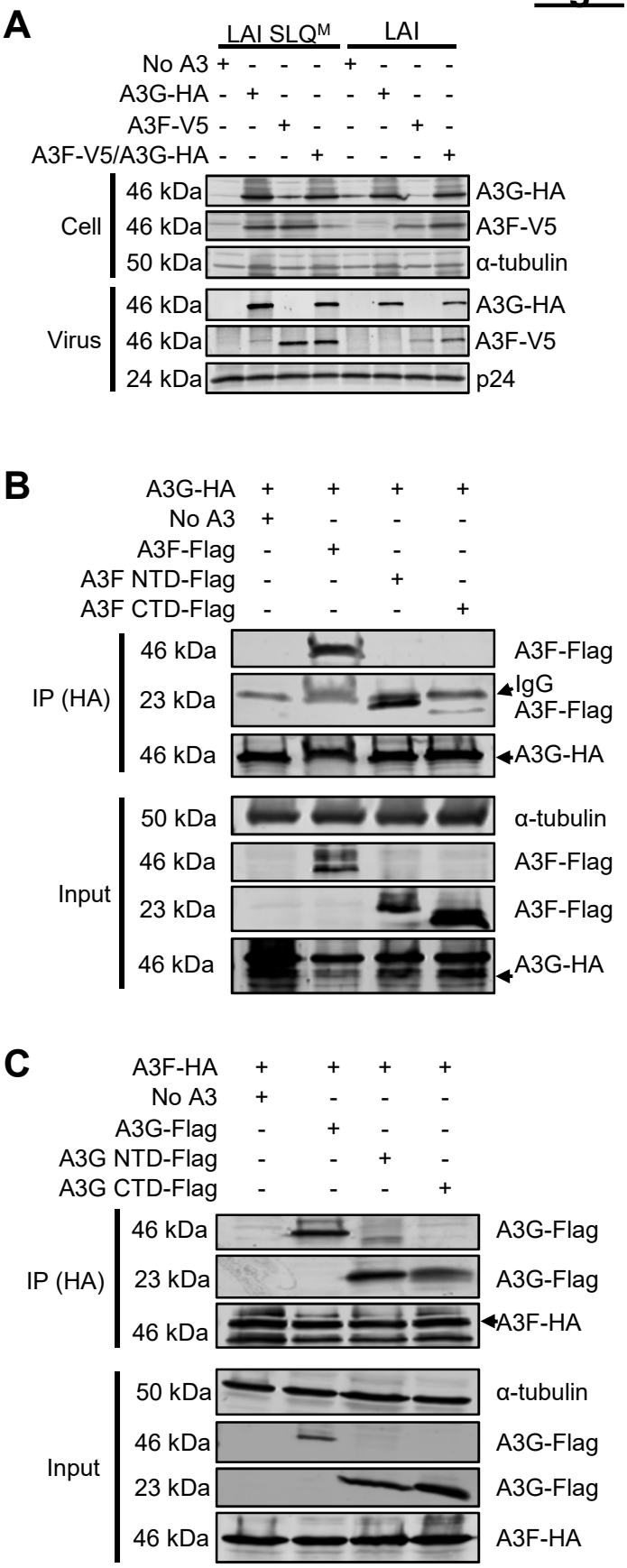
A
LAI SLQM
LAI
No A3 + - - - + - - -
A3G-HA - + - - - + - -
A3F-V5 - - + - - - + -
A3F-V5/A3G-HA - - - + - - - +
Cell
46 kDa A3G-HA
46 kDa A3F-V5
50 kDa α-tubulin
Virus
46 kDa A3G-HA
46 kDa A3F-V5
24 kDa p24
B
A3G-HA + + + +
No A3 + - - -
A3F-Flag - + - -
A3F NTD-Flag - - + -
A3F CTD-Flag - - - +
IP (HA)
46 kDa A3F-Flag
23 kDa IgG
A3F-Flag
46 kDa A3G-HA
Input
50 kDa α-tubulin
46 kDa A3F-Flag
23 kDa A3F-Flag
46 kDa A3G-HA
C
A3F-HA + + + +
No A3 + - - -
A3G-Flag - + - -
A3G NTD-Flag - - + -
A3G CTD-Flag - - - +
IP (HA)
46 kDa A3G-Flag
23 kDa A3G-Flag
46 kDa A3F-HA
Input
50 kDa α-tubulin
46 kDa A3G-Flag
23 kDa A3G-Flag
46 kDa A3F-HA

Fig 2

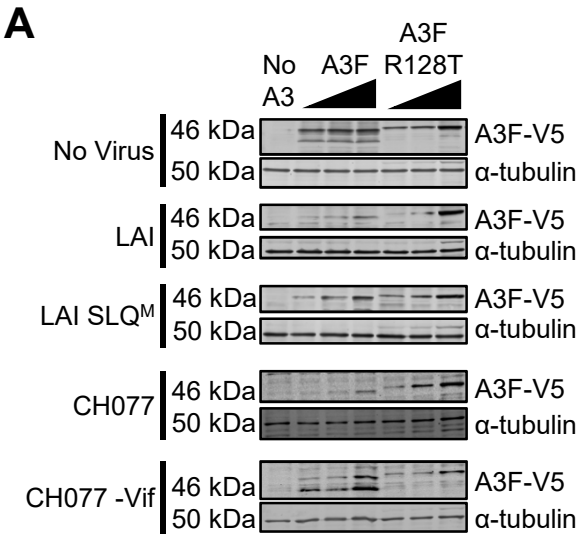
A
No A3
A3F
A3F R128T
No Virus
LAI
LAI SLQ^M
CH077
CH077 -Vif
46 kDa
50 kDa
A3F-V5
α-tubulin

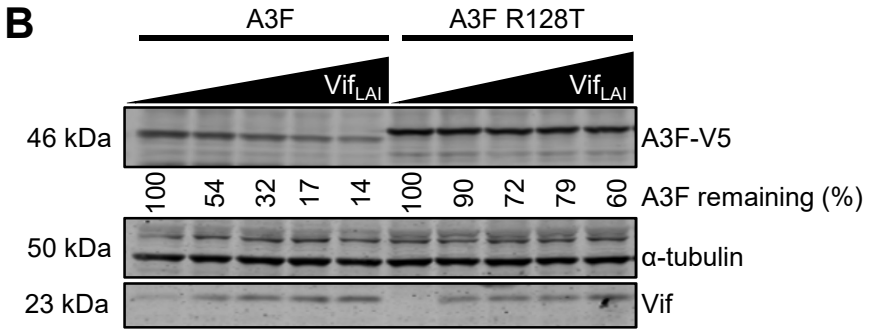
B
A3F
A3F R128T
Vif_LAI
46 kDa
A3F-V5
100
54
32
17
14
100
90
72
79
60
A3F remaining (%)
50 kDa
α-tubulin
23 kDa
Vif

Fig 3

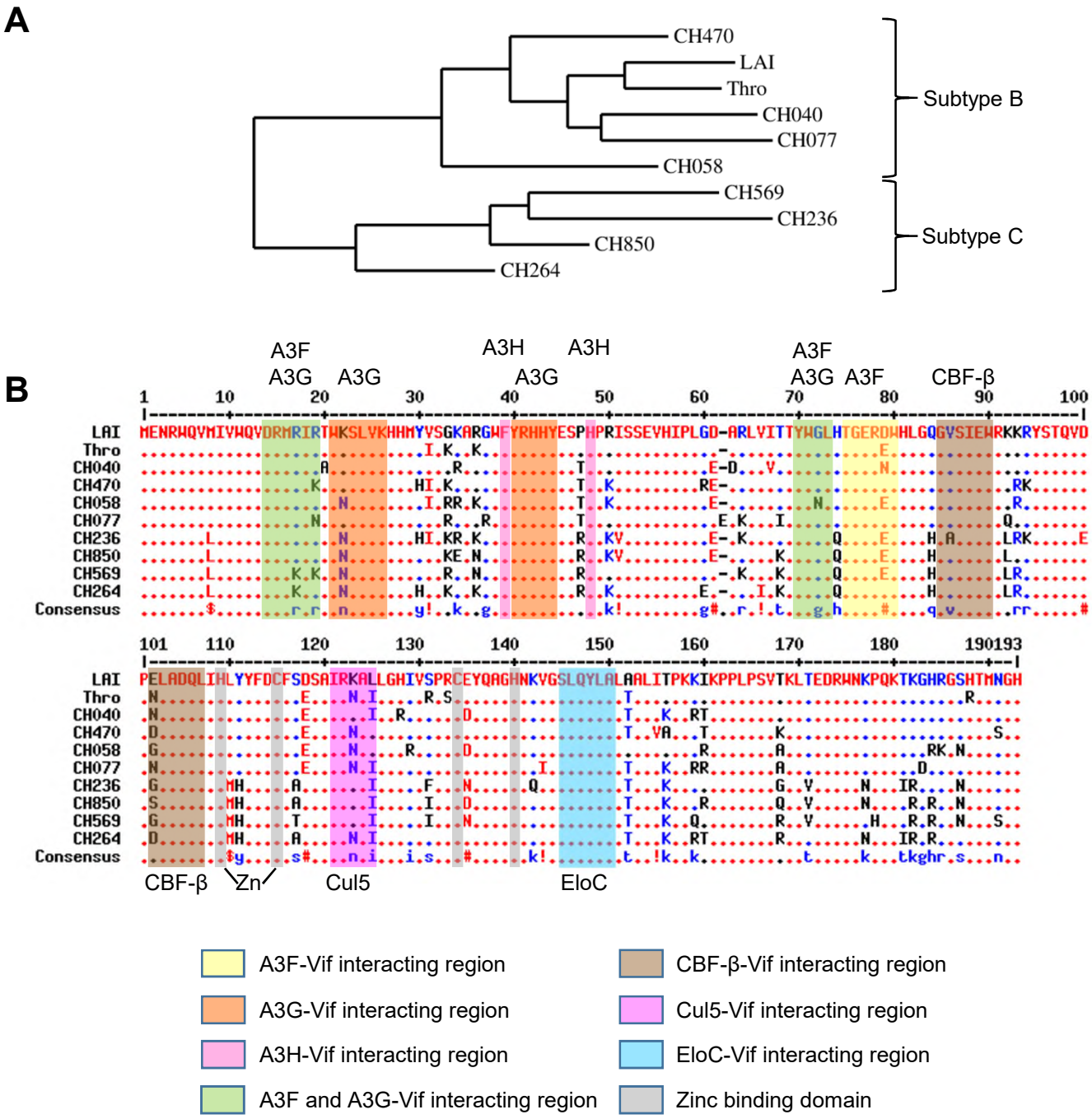
A
CH470
LAI
Thro
CH040
CH077
CH058
CH569
CH236
CH850
CH264
Subtype B
Subtype C
B
A3F
A3G
A3G
A3H
A3G
A3H
A3F
A3G
A3F
CBF-β
LAI
Thro
CH040
CH470
CH058
CH077
CH236
CH850
CH569
CH264
Consensus
CBF-β
Zn
Cul5
EloC
A3F-Vif interacting region
A3G-Vif interacting region
A3H-Vif interacting region
A3F and A3G-Vif interacting region
CBF-β-Vif interacting region
Cul5-Vif interacting region
EloC-Vif interacting region
Zinc binding domain

Fig 4

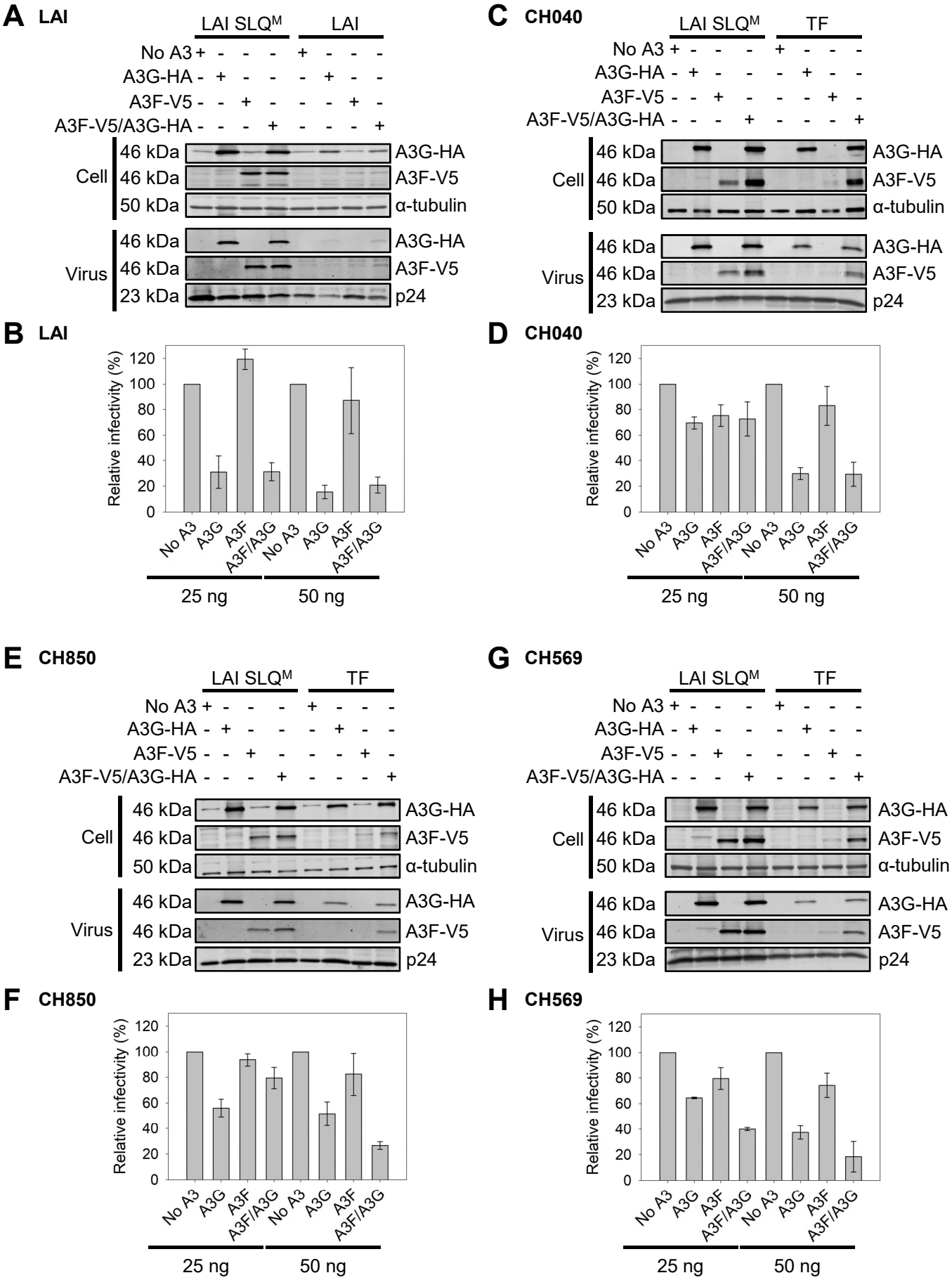
A LAI
LAI SLQM
LAI
No A3
A3G-HA
A3F-V5
A3F-V5/A3G-HA
Cell
Virus
46 kDa
50 kDa
23 kDa
A3G-HA
A3F-V5
α-tubulin
p24
B LAI
Relative infectivity (%)
No A3
A3G
A3F
A3F/A3G
25 ng
50 ng
C CH040
TF
D CH040
E CH850
F CH850
G CH569
H CH569

Fig 5

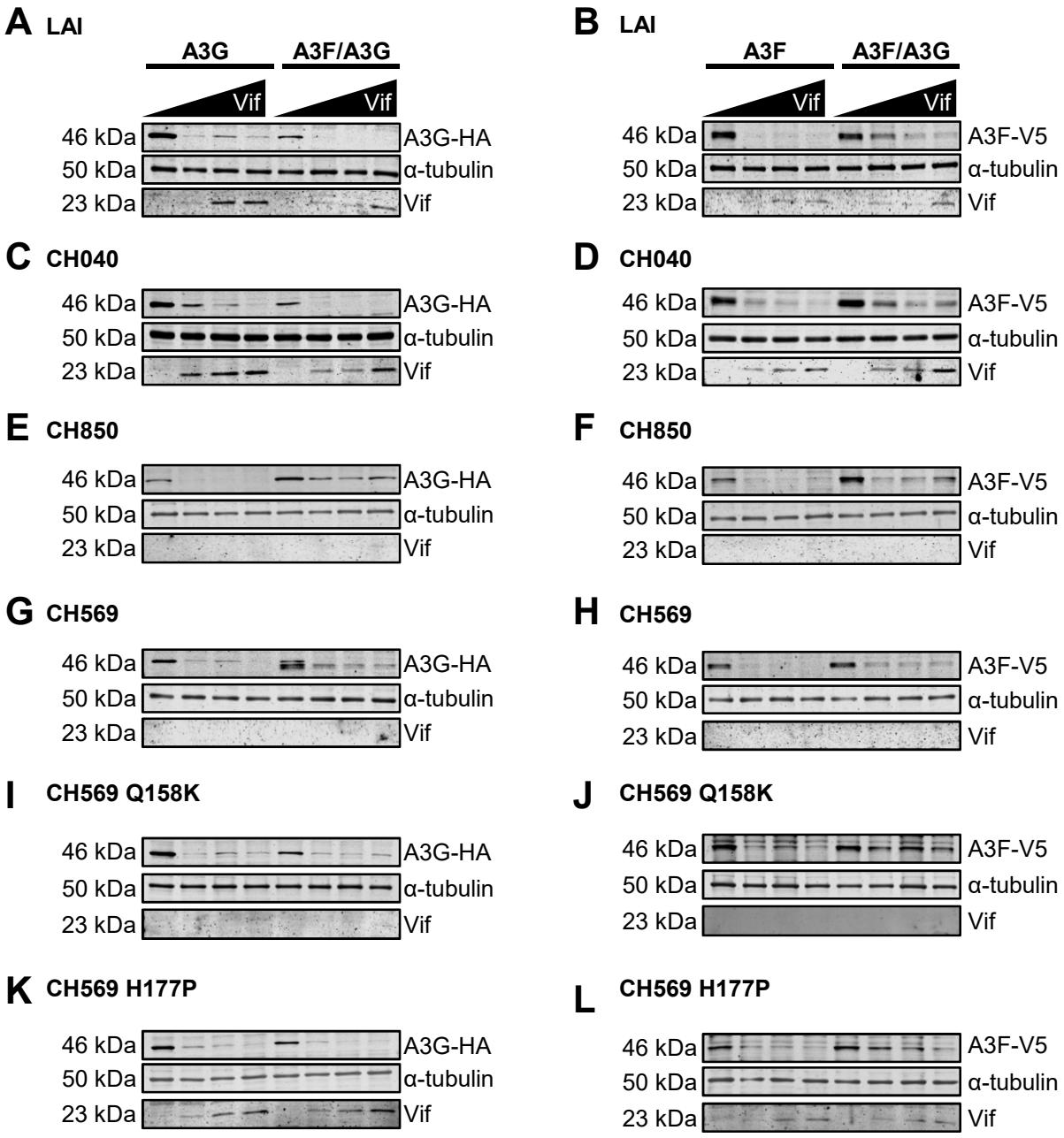
A LAI
A3G
A3F/A3G
Vif
Vif
46 kDa
50 kDa
23 kDa
A3G-HA
α-tubulin
Vif
B LAI
A3F
A3F/A3G
Vif
Vif
46 kDa
50 kDa
23 kDa
A3F-V5
α-tubulin
Vif
C CH040
46 kDa
50 kDa
23 kDa
A3G-HA
α-tubulin
Vif
D CH040
46 kDa
50 kDa
23 kDa
A3F-V5
α-tubulin
Vif
E CH850
46 kDa
50 kDa
23 kDa
A3G-HA
α-tubulin
Vif
F CH850
46 kDa
50 kDa
23 kDa
A3F-V5
α-tubulin
Vif
G CH569
46 kDa
50 kDa
23 kDa
A3G-HA
α-tubulin
Vif
H CH569
46 kDa
50 kDa
23 kDa
A3F-V5
α-tubulin
Vif
I CH569 Q158K
46 kDa
50 kDa
23 kDa
A3G-HA
α-tubulin
Vif
J CH569 Q158K
46 kDa
50 kDa
23 kDa
A3F-V5
α-tubulin
Vif
K CH569 H177P
46 kDa
50 kDa
23 kDa
A3G-HA
α-tubulin
Vif
L CH569 H177P
46 kDa
50 kDa
23 kDa
A3F-V5
α-tubulin
Vif